Available online at www.sciencedirect.com

ScienceDirect

Procedia Engineering 133 (2015) 60 – 71

Procedia Engineering

www.elsevier.com/locate/procedia

6th Fatigue Design conference, Fatigue Design 2015

Multi-axial fatigue criteria with length scale and gradient effects

Ma Zepeng[a,*], Patrick Le Tallec[b], Habibou Maitournam[c]

[a]*Laboratory of Solid Mechanics, Ecole Polytechnique, 91128 Palaiseau Cedex, France*
[b]*Laboratory of Solid Mechanics, Ecole Polytechnique, 91128 Palaiseau Cedex, France*
[c]*IMSIA, ENSTA ParisTech, CNRS, CEA, EDF, Université Paris-Saclay, 828 bd des Maréchaux, 91762 Palaiseau cedex France*

Abstract

The objective of the work is first to extend some classic high cycle fatigue (HCF) criteria (as Crossland, Dang Van, Papadopoulos, ...) to take into account a sensitivity of the criteria to stress spatial variations occurring at length scale l_g, and second to compare the performances of the extensions through numerical simulations of experimental fatigue tests. After an introduction of the basic criteria and their gradient based extensions proposed by Luu et al., we focus on the Crossland criterion to propose a more practical and simple expression taking into account the gradient of the stress amplitude and the maximum hydrostatic stress. The proposition is then tested and applied to different simple situations: 4-point bending and cantilever rotative bending. The relative errors between the exact solutions and the numerical simulations are estimated. Biaxial bending-torsion tests are also simulated to demonstrate the capabilities of the approach. The generalization of the approach to other multiaxial fatigue criteria is briefly shown through the case of Papadopoulos 2001 proposal. Finally, the present study develops a simple formulation of gradient multi-axial fatigue criteria extending the classical HCF criteria. In this work only stress gradient with a beneficial effect on fatigue have been considered.

Keywords: Fatigue; Gradient; Multi-axial; High cycle; Length scale

1 Introduction

In several industries, the required design lifetime of many components often exceeds 10^8 cycles. This requirement is applicable to aircraft (gas turbine disks 10^{10} cycles), automobiles (car engine 10^8 cycles), and railways (high speed train 10^9 cycles). Although a large amount of fatigue data has been published in the form of S-N (where S is stress and N the number of cycles to fatigue) curves, the data in the literature have been usually limited to fatigue lives up to 10^7 cycles. Using traditional fatigue criteria, a near hyperbolic relationship between stress and fatigue life is assumed, with an asymptotic limit defined as the fatigue limit (or endurance stress). A large number of multiaxial fatigue criteria, generalizing this notion of fatigue limit, are available in the literature [1][2][3]. They are practically used to design industrial components against failure. Nevertheless, most of these criteria present some drawbacks, for instance when dealing with out-of-phase loading or with metals of different kinds from those used to develop the criteria. In fact, quite all of

*Corresponding author. Email address: zepeng.ma@polytechnique.edu

Peer-review under responsibility of CETIM
doi:10.1016/j.proeng.2015.12.624

them are not designed to cope with high stress gradient introducing by surface treatments or notches, and also with scale effect especially present in nano or micro components.

More precisely, as mentioned by Luu et al. [4], in problems related to small electronic components and electro-mechanical devices, at sufficiently small sizes, factors as size, gradient and loading effects affecting fatigue limits are not captured by classical fatigue criteria. The general statement "the smaller the size, the higher the gradient, then the higher fatigue resistance" sums up the following observations.

Loading effects: the three types of tests with different volumes of the most loaded zones are examined in [4]. In descending volume order, they are tension-compression, rotative bending and plane bending, leading to increasing order of fatigue limits.

Size: for the same in-state stress distribution as well as nominal maximum stress and material, the smaller the sample size is, the smaller the surface or the volume of the most stressed zone is, the higher the fatigue limit is.

Stress gradient: the nominal fatigue limit increases in the presence of stress gradient corresponding to a decreasing stress from the surface. Experimental example illustrates and makes clearer "beneficial gradient effect" [5]. The results of the constant moment tests on specimens of the same radius but different lengths shows that the gradient effect is an order of magnitude higher than the pure size effect. In this case, size effect is proved insignificant compared to the gradient effect at the considered scale.

From above it is concluded that the stress gradient factor is the most important contributer to this phenomenon. It has been generalized by several authors to include a gradient dependence [5] in order to introduce a sensitivity of the endurance limit to space variations occurring at length scale l_g. Uniaxial normal cyclic stress states with non-zero and zero normal stress gradients, respectively, allow drawing some comments about the normal stress gradient effect. The larger the normal stress due to bending, the larger the difference between bending test points and tension-compression ellipse arc (as is shown in Fig. 1).

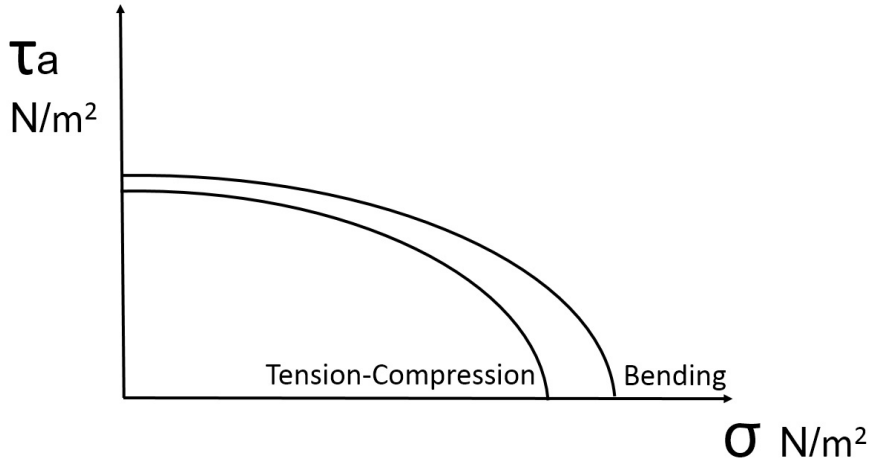

Fig. 1: Schematic representation of the nominal fatigue limit (ellipse arc) for two different tests: the arc is larger in the case of bending-torsion (presence of stress gradient) than in tension-compression.

Apart from gradient approaches[6][5], to take account of these effect, others approaches such critical volume [7], critical distance[8][9], critical layer[10], averaging over a specific volume [11][12] are used . In fact, all the approaches are equivalent to introducing a length scale. In the paper, we consider specifically the gradient approach. We start from the proposition of Luu et al., and propose and a simpler way to account for the gradient. The Crossland criterion, one of the most widely known HCF criteria, is used to illustrate the approach. Crossland proposed that the second invariant of the deviatoric stress tensor and the hydrostatic stress are the variables governing the endurance limit. The new proposition adds two gradient terms ; it is then calibrated and its predictions are compared to experimental results to check its relevancy.

2 Approach of Luu et al.

2.1. General formulation

Luu et al. [4] proposed extensions of classical HCF fatigue criteria using the gradients of the shear and normal stress to account for the gradient effect. In the case of critical plane type criteria, they defined a generalized shear stress amplitude including shear stress gradient and a generalized maximum normal (or hydrostatic) stress. A general form of classical fatigue limit criteria can be written as follows:

$$f(C_a(n^*), N_{max}(n^*)) = C_a(n^*) + aN_{max}(n^*) - b \geqslant 0, \tag{1}$$

with a, b being two material parameters. f is a function, chosen in many cases as linear, and n^* is the normal vector of the critical plane; $C_a(n^*)$, $N_{max}(n^*)$ are respectively the amplitude of shear stress and the maximum value of the normal stress on the critical plane.

A new class of fatigue criteria extended from classical ones with stress gradient terms introducing not only in the normal stress but also in the shear stress components, was proposed. It concerns only free defect materials and can model both phenomena "smaller is Stronger and Higher Gradient is Stronger".

Besides the stress gradient term appearing in the normal stress part in form of $G = \Delta(\sigma_{11} + \sigma_{22} + \sigma_{33})$, another gradient term, the gradient of the stress tensor amplitude (or alternatively of deviatoric stress tensor amplitude) $\| Y_a \| = \Delta\sigma_a$ is added to the shear stress amplitude part. Basing on all these analyses a new form of fatigue criteria taking into account gradient effects, is proposed:

$$f(\widetilde{C_a}(n^*), \widetilde{N_{max}}(n^*)) = \widetilde{C_a}(n^*) + a\widetilde{N}_{max}(n^*) - b \geqslant 0, \tag{2}$$

where $\widetilde{C_a}(n^*)$ and $\widetilde{N_{max}}(n^*)$ are extended definitions of the amplitude of shear stress and of the normal stress taking into account the presence of local gradient.

In the following we just focus on the Crossland criterion and its extension.

2.2. Recall of the classical Crossland criterion

The classical Crossland criterion defines the fatigue limit of metallic specimens subjected to multi-axial cyclic stress[13] :

$$f(\sqrt{J_{2,a}}, P_{max}) = \sqrt{J_{2,a}} + aP_{max} - b \leqslant 0 \tag{3}$$

where $\sqrt{J_{2,a}}$ measures the amplitude of variation of the second invariant of the deviatoric stress and P_{max} is the maximum hydrostatic stress observed during a loading cycle. The parameters a and b are material constants to be calibrated experimentally. The amplitude of the square root of the second invariant of the stress deviator can be defined, in general case, as the half-length of the longest chord of the deviatoric stress path or as the radius of the smallest hypersphere circumscribing the stress deviator loading path [1]

$$\sqrt{J_{2,a}} = \frac{1}{2\sqrt{2}} \min_{\underline{\underline{S}}_1} \{\max_t \sqrt{(\underline{\underline{S}}(t) - \underline{\underline{S}}_1) : (\underline{\underline{S}}(t) - \underline{\underline{S}}_1)}\} \tag{4}$$

The deviatoric stress $\underline{\underline{S}}$ associated with a stress tensor $\underline{\underline{\sigma}}$ is defined by

$$\underline{\underline{S}} = \underline{\underline{\sigma}} - \frac{1}{3}\mathrm{tr}\underline{\underline{\sigma}}\,\underline{\underline{I}} \tag{5}$$

where $\mathrm{tr}\underline{\underline{\sigma}}$ is the trace of the stress tensor $\underline{\underline{\sigma}}$ and $\underline{\underline{I}}$ the second order unit tensor.

The maximum value that the hydrostatic stress reaches during the loading cycle is on the other hand:

$$P_{max} = \max_t \{\frac{1}{3}\mathrm{tr}(\underline{\underline{\sigma}}(t))\}. \tag{6}$$

For a proportional cyclic loading, if one introduces the two extreme stress tensors $\underline{\underline{\sigma}}^A$ and $\underline{\underline{\sigma}}^B$ observed during the loading path, together with the stress range

$$\Delta\underline{\underline{\sigma}} = \underline{\underline{\sigma}}^B - \underline{\underline{\sigma}}^A \tag{7}$$

and its deviatoric part $\underline{\underline{\Delta s}}$, the variation of the second invariant of the stress deviator reduces to

$$\sqrt{J_{2,a}} = \frac{1}{2}\max_t \sqrt{\frac{1}{2}\underline{\underline{\Delta s}} : \underline{\underline{\Delta s}}} = \frac{1}{2}\max_t \sqrt{\frac{1}{2}(\Delta s_{11}^2 + \Delta s_{22}^2 + \Delta s_{33}^2 + 2\Delta s_{12}^2 + 2\Delta s_{13}^2 + 2\Delta s_{23}^2)}. \tag{8}$$

The material constants a and b can be related to the limit t_{-1} of endurance in alternate torsion and to the limit s_{-1} of endurance in alternate tension-compression by

$$a = \frac{3t_{-1}}{s_{-1}} - \sqrt{3}, \quad b = t_{-1}. \tag{9}$$

2.3. Formulation of Crossland criterion with gradient effect

In particular, using as a basis the classical Crossland criterion Eq.(3) and the general framework for the development of a gradient dependent fatigue limit criterion Eq.(2), a new version can be written in the form:

$$\sqrt{\widetilde{J_{2,a}}} + a\widetilde{P_{max}} \leqslant b. \tag{10}$$

This formula takes into account the indicator of the influence of the gradient of the stress deviator which reflects the spatial non-uniform distribution of stress state.

In practice, [4] had proposed:

$$\sqrt{J_{2,a}}\sqrt{1 - \left(l_\tau \frac{\| \underline{\underline{Y}} \|_{,a}}{\| \underline{\underline{S}} \|_{,a}}\right)^{n_\tau}} + aP_{max}\left(1 - \left\langle l_\sigma \frac{\| G \|}{P_{max}}\right\rangle^{n_\sigma}\right) - b < 0. \tag{11}$$

Here $\| \underline{\underline{Y}} \|_{,a}$ is the full stress gradient and $\| G \|$ is used as an indicator of the influence of the normal stresses gradient.

$$\| G \| = \| \nabla P_{max} \| = \sqrt{\left(\frac{\partial P_{max}}{\partial x}\right)^2 + \left(\frac{\partial P_{max}}{\partial y}\right)^2 + \left(\frac{\partial P_{max}}{\partial z}\right)^2}. \tag{12}$$

3 Optimized Crossland Criterion formulation

The precedent Luu and al. formula has six materials parameters a,b,l_τ,l_σ,n_τ,n_σ to be identified experimentally. The calibration can be complicated ; it does not lead to a unique set of parameters. Physical considerations, such as the length scales, have to be taken into account for choosing the optimized material constants. For practical application in an industrial context, it is essential to reduce the number of parameters. We therefore wish to investigate a simpler construction, departing from the classical Crossland criterion.

Surfaces with stresses decreasing in depth are, here and after, considered. Failure occurs at the point x_0 when, $(\sqrt{J_{2,a}} + aP_{max} - b)(x_0) \geqslant 0$. To be more general and avoid singularity, this condition should be satisfied in some x_0 neighboring volume of size l_g, leading to a criterion given by:

$$\inf_{\underline{x} \in B(\underline{x_0}, \underline{l_g})} (\sqrt{J_{2,a}} + aP_{max} - b)(x) \geqslant 0. \tag{13}$$

To obtain a suitable expression, an expansion of Eq.(13) in performed in the neighborhood of x_0. The sought formula should account for the beneficial effect of the stress gradient. Considering that the stress is decreasing in depth, a negative sign is associated with the norm of the gradient of stress tensor in to the proposed formula. In addition, the gradient term should not only affect hydrostatic stress but also shear stress.

An objective formulation based on the lowest possible value of $\sqrt{J_{2,a}}$ and of P_{max} in the neighborhood, is finally:

$$\sqrt{J_{2,a}} + aP_{max} - l_g \parallel \nabla \sqrt{J_{2,a}} + a\nabla P_{max} \parallel \leqslant b, \tag{14}$$

We keep the same material parameters a and b as before. l_g is a characteristic length to be optimized to match the experimental results. The approach has only one supplementary material constant whose calibration is easy.

4 Calibration of the criterion

In this section, two different uniaxial fatigue tests with stress gradient effects are used to calibrate the optimized gradient Crossland criterion. An application to a biaxial test fatigue test shows the ability of the proposed approach to account the stress gradient in multiaxial cases.

4.1. Fully reversed 4-point bending and rotating cantilever bending fatigue tests

The model of 4-point bending is first considered. The bar made of steel has both ends fixed. The radius R is a variable ranging from 1mm to 30mm enough to highlight the fact "the smaller, the stronger". The length L of the bar is 100 mm.

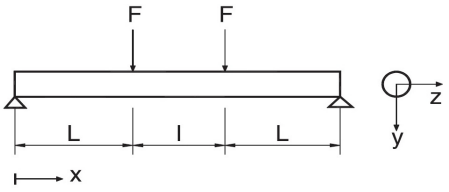

Fig. 2: 4-point bending test [14]

The bending moment is the same in the interval $L \leqslant x \leqslant L + l$ and equal to $M = FL$ (Fig. 2). The bending stress $\boldsymbol{\sigma}$ and its gradient $\mathbf{Y}$ for $L \leqslant x \leqslant L + l$ and $-R \leqslant y \leqslant R$ are then:

$$\underline{\underline{\sigma}} = \sigma_{xx} sin(wt) e_x \otimes e_x = \frac{FLy}{I} sin(wt) e_x \otimes e_x$$

with $I = \frac{\pi R^4}{4}$
The maximum stress during the cyclic loading in the bar is: $\sigma_{max} = \frac{FLy}{I}$.
The gradient components of $\mathbf{Y}$ is: $\sigma_{xx,x} = 0, \sigma_{xx,y} = \frac{FL}{I} = \frac{\sigma_{max}}{y}, \sigma_{xx,z} = 0$.
The macroscopic stress range is: $\underline{\underline{\Delta\sigma}}(t) = 2\sigma_{max} e_x \otimes e_x$ The hydrostatics stress:

$$P_{max} = \max_t \{\frac{1}{3}\mathrm{tr}(\sigma(t))\} = \frac{1}{3}\sigma_{max} = \frac{FLy}{3I}, \tag{15}$$

Deviator of the macroscopic stresses:

$$\underline{\underline{\Delta S}} = \underline{\underline{\Delta\sigma}} - \frac{1}{3}\mathrm{tr}\underline{\underline{\Delta\sigma I}} = \begin{pmatrix} \frac{4}{3}\sigma_{max} & 0 & 0 \\ 0 & -\frac{2}{3}\sigma_{max} & 0 \\ 0 & 0 & -\frac{2}{3}\sigma_{max} \end{pmatrix}. \tag{16}$$

The second invariant of the stress deviator is then:

$$\sqrt{J_{2,a}} = \frac{1}{2\sqrt{2}} \sqrt{\underline{\underline{\Delta S}} : \underline{\underline{\Delta S}}} = \frac{\sigma_{max}}{\sqrt{3}} = \frac{FLy}{\sqrt{3}I}. \tag{17}$$

Then the gradient part has the value:

$$\nabla \sqrt{J_{2,a}} = \frac{\partial \sqrt{J_{2,a}}}{\partial x}\underline{e}_x + \frac{\partial \sqrt{J_{2,a}}}{\partial y}\underline{e}_y + \frac{\partial \sqrt{J_{2,a}}}{\partial z}\underline{e}_z = (0, \frac{FL}{\sqrt{3}I}, 0), \tag{18}$$

and

$$\nabla P_{max} = (0, \frac{FL}{3I}, 0). \tag{19}$$

The parameters a and b of the standard Crossland criterion, are obtained from fully reversed tension-compression fatigue limit s_{-1} and torsion fatigue limit t_{-1} using Eq.(9).

From Eq.(3), standard Crossland criterion without gradient effect (for radius R) is:

$$\sqrt{J_{2,a}} + aP_{max} = \frac{FLR}{\sqrt{3}I} + \frac{aFLR}{3I} \leqslant b. \tag{20}$$

The gradient term here is given by:

$$\| \nabla \sqrt{J_{2,a}} + a\nabla P_{max} \| = \frac{FL}{\sqrt{3}I} + \frac{aFL}{3I}. \tag{21}$$

By comparison we can see in 4-point bending test the difference between classical and modified Crossland criterion is related to the product of the characteristic length l_g and the term (21) associated to the decrease of the stress in depth. This value shows how much the modification affects the Crossland criterion. Crossland criterion with beneficial gradient term as shown in Eq.(14) is given by:

$$\begin{aligned} \sqrt{J_{2,a}} + aP_{max} - l_g(\| \nabla \sqrt{J_{2,a}} + a\nabla P_{max} \|) = \\ \frac{FLR}{\sqrt{3}I} + \frac{aFLR}{3I} - l_g(\frac{FL}{\sqrt{3}I} + \frac{aFL}{3I}) = \\ \frac{1}{\sqrt{3}}\sigma_{max} + \frac{a}{3}\sigma_{max} - l_g(\frac{1}{\sqrt{3}R}\sigma_{max} + \frac{a}{3R}\sigma_{max}) \leqslant b\,, \end{aligned} \tag{22}$$

which is to say:

$$\sigma_{max} \leqslant \frac{b}{\frac{1}{\sqrt{3}} + \frac{a}{3} - l_g(\frac{1}{\sqrt{3}R} + \frac{a}{3R})}\,. \tag{23}$$

The material parameters a and b are obtained using their classical expressions as Eq.(9) from tests free of stress gradient. The corresponding fatigue limit are denoted s_{ref} for the alternate tension-compression test, and t_{ref} for the alternate torsion test. For a specimen of radius R the alternate bending fatigue limit is denoted $f(R)$. We can observe that:

$$f(R) = \frac{b}{\frac{1}{\sqrt{3}} + \frac{a}{3} - l_g(\frac{1}{\sqrt{3}R} + \frac{a}{3R})} \geqslant s_{ref} \tag{24}$$

$f(R)$ tends to s_{ref} for large radii.

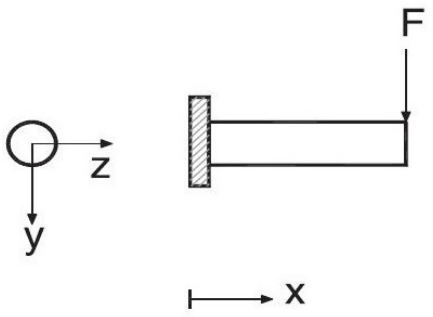

Fig. 3: Cantilever bending test [14]

In the case of cantilever fully reversed bending. Let us denote the corresponding fatigue limit by σ_{max}. The second invariant of the stress deviator is then:

$$\sqrt{J_{2,a}} = \frac{1}{2\sqrt{2}} \sqrt{\underline{\underline{\Delta S}} : \underline{\underline{\Delta S}}} = \frac{\sigma_{max}}{\sqrt{3}}. \tag{25}$$

The hydrostatics stress:

$$P_{max} = \max_t \{\frac{1}{3}\mathrm{tr}(\sigma(t))\} = \frac{1}{3}\sigma_{max}. \tag{26}$$

Which results in the same gradient terms as in 4-point bending.

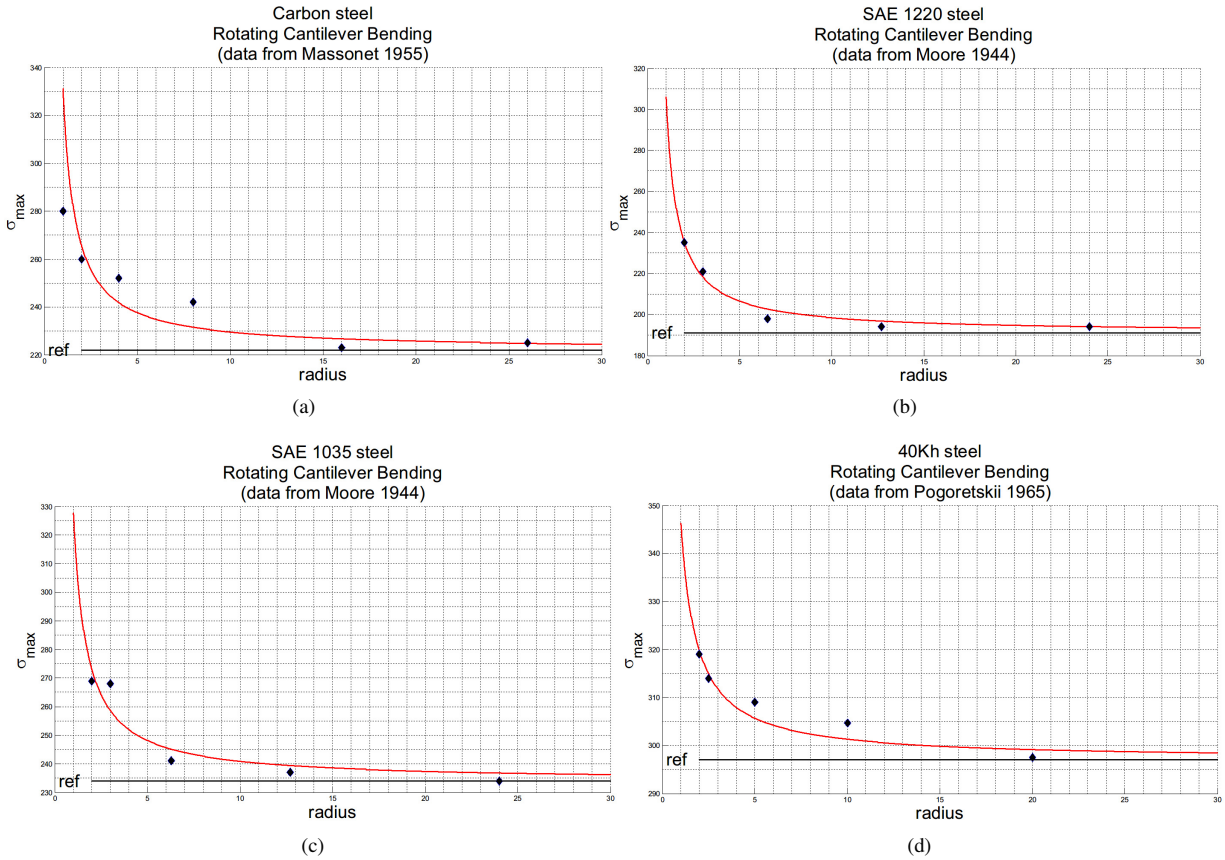

Fig. 4: Fatigue limits with gradient effect for different radii.

Eq.(24) with a et b calibrated from given S_{ref} and t_{ref} is used to estimate the characteristic length l_g in order to give the best correlation between simulated and experimental fatigue limit obtained in rotating cantilever bending tests for different materials and radii. The results are sketched in Fig.(4).
The fatigue limit of carbon steel is in alternate torsion is $t_{ref} = 151MPa$ and the fatigue limit in alternate tension-compression is $s_{ref} = 222MPa$. After fitting, we get $l_g = 0.3297$.
The fatigue limit of SAE 1220 steel is in alternate torsion is $t_{ref} = 143MPa$ and the fatigue limit in alternate tension-compression is $s_{ref} = 191MPa$.After fitting, we get $l_g = 0.3755$.
The fatigue limit of SAE 1035 steel is in alternate torsion is $t_{ref} = 172MPa$ and the fatigue limit in alternate tension-compression is $s_{ref} = 234MPa$. After fitting, we get $l_g = 0.2861$.
The fatigue limit of 40Kh steel is in alternate torsion is $t_{ref} = 180MPa$ and the fatigue limit in alternate tension-compression is $s_{ref} = 297MPa$. After fitting, we get $l_g = 0.1424$.

We can observe a very interesting phenomenon that the smaller fatigue limit is, the larger influence of gradient effect is.

Table 1: Length scales of different materials

	1220 steel	Carbon steel	1035 steel	40Kh steel
S_{ref} [MPa]	191	222	234	297
t_{ref} [MPa]	143	151	172	180
l_g [mm]	0.3755	0.3297	0.2861	0.1424

4.2. Bending-torsion fatigue tests

The bending moment is a linear function of x, $M_b = -F(L-x)$. The twisting moment is denoted M_t. The stress σ_{xx} now varies along the depth (i.e. y-axis) and the length (i.e. x-axis) of the specimen. Consequently, the gradient of σ_{xx} has two non-zero components, the derivatives with respect to x and y. Considering the critical points (located at $y = \pm R$) The bending stress and its gradient for $0 \leqslant x \leqslant L$ are given by the formulas:

$$\sigma_a = \frac{-F(L-x)}{I} R = \frac{M_b}{I} y \tag{27}$$

with $I = \frac{\pi R^4}{4}$, $\tau_a = \frac{M_t}{J} y$ and $J = \frac{1}{2}\pi R^4$. The stress tensor $\underline{\underline{\sigma}}$ is then:

$$\underline{\underline{\sigma}}(t) = \begin{pmatrix} \sigma_a sin(\omega t) & \tau_a sin(\omega t) & 0 \\ \tau_a sin(\omega t) & 0 & 0 \\ 0 & 0 & 0 \end{pmatrix}. \tag{28}$$

The stress range tensor is:

$$\underline{\underline{\Delta\sigma}} = \begin{pmatrix} 2\sigma_a & 2\tau_a & 0 \\ 2\tau_a & 0 & 0 \\ 0 & 0 & 0 \end{pmatrix}. \tag{29}$$

Deviator of the macroscopic stresses:

$$\underline{\underline{\Delta S}} = \underline{\underline{\Delta\sigma}} - \frac{1}{3}\mathrm{tr}\underline{\underline{\Delta\sigma}} = \begin{pmatrix} \frac{4}{3}\sigma_a & 2\tau_a & 0 \\ 2\tau_a & -\frac{2}{3}\sigma_a & 0 \\ 0 & 0 & -\frac{2}{3}\sigma_a \end{pmatrix}. \tag{30}$$

The second invariant of the stress deviator is then:

$$\sqrt{J_{2,a}} = \frac{1}{2\sqrt{2}} \sqrt{\underline{\underline{\Delta S}} : \underline{\underline{\Delta S}}} = \sqrt{\frac{1}{3}\sigma_a^2 + \tau_a^2} = \sqrt{\frac{M_b^2}{3I^2} + \frac{M_t^2}{4J^2}}\, y. \tag{31}$$

The hydrostatics stress:

$$P_{max} = \max_t\{\frac{1}{3}\mathrm{tr}(\sigma(t))\} = \frac{\sigma_a}{3} = \frac{M_b}{3I} y, \tag{32}$$

Then the gradient part has the value:

$$\begin{aligned} \nabla\sqrt{J_{2,a}} = \frac{\partial\sqrt{J_{2,a}}}{\partial x}\underline{e}_x + \frac{\partial\sqrt{J_{2,a}}}{\partial y}\underline{e}_y + \frac{\partial\sqrt{J_{2,a}}}{\partial z}\underline{e}_z &= (0, \sqrt{\frac{M_b^2}{3I^2} + \frac{M_t^2}{4J^2}}, 0) \\ &= (0, \frac{\sqrt{\frac{1}{3}\sigma_a^2 + \tau_a^2}}{y}, 0), \end{aligned} \tag{33}$$

and

$$\nabla P_{max} = (0, \frac{M_b}{3I}, 0) = (0, \frac{\sigma_a}{3y}, 0). \tag{34}$$

The parameters a and b of the standard Crossland criterion, are obtained from fully reversed tension-compression fatigue limit s_{ref} and torsion fatigue limit t_{ref} using Eq.(9).
From Eq.(3), standard Crossland criterion without gradient effect writes:

$$\sqrt{J_{2,a}} + aP_{max} = \sqrt{\frac{\sigma_a^2}{3} + \tau_a^2} + \frac{\sigma_a}{3} \leqslant b. \tag{35}$$

The gradient term here is given by:

$$\| \nabla \sqrt{J_{2,a}} + a\nabla P_{max} \| = \frac{\sqrt{\frac{\sigma_a^2}{3} + \tau_a^2}}{y} + \frac{a\sigma_a}{3y}. \tag{36}$$

Crossland criterion with beneficial gradient term as shown in Eq.(14):

$$\begin{aligned} &\sqrt{J_{2,a}} + aP_{max} - l_g(\| \nabla \sqrt{J_{2,a}} + a\nabla P_{max} \|) = \\ &\sqrt{\frac{\sigma_a^2}{3} + \tau_a^2} + \frac{a\sigma_a}{3} - l_g\left(\frac{\sqrt{\frac{\sigma_a^2}{3} + \tau_a^2}}{y} + \frac{a\sigma_a}{3y}\right) \leqslant b \end{aligned} \tag{37}$$

This ellipse arc delimits in the $s_{ref} - t_{ref}$ plane the safe domain against fatigue failure(the blue arc). Clearly, Eq. (35) is the Crossland criterion for combined normal and shear stress. However, if one tries to predict the behavior of the material in combined bending and torsion, which involves the gradients of normal and shear stresses, high discrepancies between predictions and experimental data will be found.

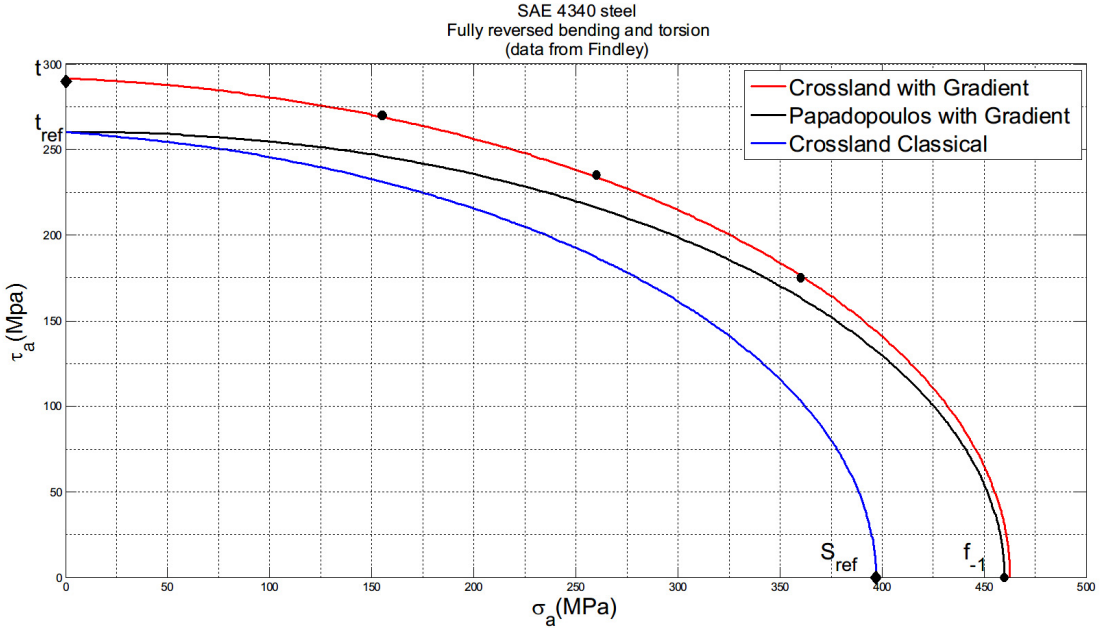

Fig. 5: Fully reversed combined bending-twisting fatigue limit data (Findley et al.[15], Papadopoulos and Panoskaltsis[14]).

By introducing the values of $\sqrt{J_{2,a}}$ and P_{max} in the the classical Crossland criterion, along with the change of parameter a from $\left(\frac{3t_{-1}}{s_{-1}} - \sqrt{3}\right)$ to $\left(\frac{3t_{-1}}{f_{-1}} - \sqrt{3}\right)$ in Eq.(3), we obtain the "Papadopoulos ellipse arc" equation in the plane of amplitudes σ_a and τ_a (the black arc):

$$\left(\frac{\tau_a}{t_{-1}}\right)^2 + \left(\frac{2f_{-1}}{\sqrt{3}t_{-1}} - 1\right)\left(\frac{\sigma_a}{f_{-1}}\right)^2 + \left(2 - \frac{2f_{-1}}{\sqrt{3}t_{-1}}\right)\frac{\sigma_a}{f_{-1}} \leqslant 1 \tag{38}$$

Our proposal takes into account both gradients of hydrostatic stress and shear stress. Choosing the proper l_g allows us to predict the experiments within the acceptable range as shown in Fig. 5 (the red arc). These results illustrate that our proposal is quite satisfactory in biaxial case.

5 Discussion

Remark 1 (Gradient terms). In this paper, the pure size effect has not been considered and only stress gradient effect is modeled.

Remark 2 (Material characteristic length scale l_g). We study here the fatigue limit of macroscopic specimens and components for which the crack initiation is generally detected by loss of stiffness corresponding to crack length which can reach a millimeter. We choose l_g ranging from 0.1 to 0.5mm. To verify the relevancy of this choice, we need more experimental data.

Remark 3 (Extensions to other criteria). The extension of the proposition to other fatigue criteria is straightforward. For instance, the modified Papadopoulos criterion [16] is written as :

$$\max T_a + a_p P_{max} - l_g \parallel \nabla\{\max T_a\} + a_p \nabla P_{max} \parallel \leqslant b_p. \tag{39}$$

6 Conclusion

The present study develops a simple formulation of gradient multi-axial fatigue criteria extending the classical HCF criteria. The objective is to model the surface gradient effects (yielding apparent size and loading effects), which is not included yet in classical mechanics but become important at small scale or in the presence of notches, by taking into account just the gradient effect. Besides, for notched fatigue problems, this approach may be still applicable.

Nevertheless, in this work only simple fatigue tests have been examined. In these tests, the gradient has a beneficial effect on fatigue. However, cases where the effect can be presumably negative, especially under the circumstances of residual stresses, can be encountered. A reexamination and validation for complex loading could be perspective for this research direction.

References

[1] Ioannis V. Papadopoulos, Piermaria Davoli, Carlo Gorla, Mauro Filippini, and Andrea Bernasconi. A comparative study of multiaxial high-cycle fatigue criteria for metals. International Journal of Fatigue, 19(3):219 – 235, 1997.

[2] P Ballard, K Dang Van, A Deperrois, and YV Papadopoulos. High cycle fatigue and a finite element analysis. Fatigue & Fracture of Engineering Materials & Structures, 18(3):397–411, 1995.

[3] Subra Suresh. Fatigue of materials. Cambridge university press, 1998.

[4] DH Luu, MH Maitournam, and QS Nguyen. Formulation of gradient multiaxial fatigue criteria. International Journal of Fatigue, 2013.

[5] Ioannis V. Papadopoulos and Vassilis P. Panoskaltsis. Invariant formulation of a gradient dependent multiaxial high-cycle fatigue criterion. Engineering Fracture Mechanics, 55(4):513 – 528, 1996.

[6] R. Amargier, S. Fouvry, L. Chambon, C. Schwob, and C. Poupon. Stress gradient effect on crack initiation in fretting using a multiaxial fatigue framework. International Journal of Fatigue, 32(12):1904 – 1912, 2010.

[7] Mahaman Habibou Maitournam, Ky Dang Van, and Jean-François Flavenot. Fatigue design of notched components with stress gradients and cyclic plasticity. Advanced Engineering Materials, 11(9):750–754, 2009.

[8] David Taylor. The theory of critical distances: a new perspective in fracture mechanics. Elsevier, 2010.

[9] J.A. Arajo, L. Susmel, D. Taylor, J.C.T. Ferro, and E.N. Mamiya. On the use of the theory of critical distances and the modified whler curve method to estimate fretting fatigue strength of cylindrical contacts. International Journal of Fatigue, 29(1):95 – 107, 2007.

[10] JF Flavenot and N Skalli. Lépaisseur de couche critique ou une nouvelle approche du calcul en fatigue des structures soumisesa des sollicitations multiaxiales. Mec. Mater. Electr, 397:15–25, 1983.

[11] T Palin-Luc. Stress gradient and size effects in multiaxial fatigue. Materials Week (Munich, Germany), 2000.

[12] A. Banvillet, T. Palin-Luc, and S. Lasserre. A volumetric energy based high cycle multiaxial fatigue citerion. International Journal of Fatigue, 25(8):755 – 769, 2003.

[13] Crossland B. Effect of large hydrostatic pressures on the torsional fatigue strength of an alloy steel. In: Proceedings of the Inter-national Conference on Fatigue of Metals, Institution of Mechan-ical Engineers, London., pages 138–149, 1956.

[14] Ioannis V Papadopoulos and Vassilis P Panoskaltsis. Invariant formulation of a gradient dependent multiaxial high-cycle fatigue criterion. Engineering Fracture Mechanics, 55(4):513–528, 1996.

[15] William Nichols Findley, JJ Coleman, and BC Hanley. Theory for Combined Bending and Torsion Fatigue with Data for SAE4340 Steel. Division of Engineering, Brown University, 1956.

[16] Ioannis V Papadopoulos. Long life fatigue under multiaxial loading. International Journal of Fatigue, 23(10):839–849, 2001.